POOL MONITORING IN GMAW

S. C. Absi Alfaro[1*], G. C. de Carvalho[1] and J.M. Motta[1]

[1]Department of Mechanical Engineering, GRACO, The Brasilia University, UnB.
Campus Universitario, 70910-900, Brasilia, DF, Brazil. sadek@graco.unb.br

ABSTRACT.

This paper describes a weld pool monitoring technique, which is based on the weld pool image analysis. The proposed image analysis algorithm uses machine vision techniques to extract geometrical information from the weld pool image such as maximum weld pool width, gap width and misalignment between the joint longitudinal axis and the welding wire. These can be related to the welding parameters (welding voltage and current, wire feed speed and standoff) to produce control actions necessary to ensure that the required weld quality will be achieved. The experiments have shown that the algorithm is able to produce good estimates of the weld pool geometry; however, the adjustment of the camera parameters affects the image quality and, consequently, has a great influence over the estimation.

KEYWORDS

Weld pool monitoring, GMA Welding Process, Weld Pool Shape.

1. Introduction

The demand for larger productivity and the shortage of qualified welders has been promoting a significant increase in the robots' use in arc and resistance welding processes. Among the arc welding processes stands out GMAW (Gas Metal Arc Welding), which use has increased in the last years due to its inherent flexibility [1 and 2]; however, it has been observed limitations in the automation processes. Overall, in the case of continuous welding, has been observed limitations essentially due to the difficulty of guaranteeing perfect alignment between the wire traveling welding path and the welding joint axis and moreover, guarantee the geometry of the weld bead, even with joint variations [2 and 3]. In the GMAW process, the levels of tolerance for preparation of welding joint as well as for positioning in actual welding are very superior for those demanded in the case of manual welding [4, 5 and 6]. For that reason, it is necessary to use monitoring systems in order to guarantee the quality of the produced welding joint in accordance with pre-established patterns, which characteristics satisfy the requirements of continuity, dimensions, mechanical resistance and in some cases aesthetic requirements [7].

The objective of this work was to develop a method of monitoring the molted weld pool through the visualization and analysis of its image; measuring such parameters as maximum weld pool width, gap width and position. These data can be related with the welding parameters (voltage, current, wire feed speed and stand off), in such way to obtain, enough information to make possible forecast the formation defects that could compromise the welding joint quality [8].

2. Weld pool monitoring.

The weld pool monitoring is usually undertaken by using vision systems and image recognition algorithms. Figure 1, shows a weld pool frontal image, where its main components can be visualized: in the most luminous part, the arc; sharply dark in the central part of the image, the wire; in intermediate gray tones, the pool; and the gap, that turns visible due to the molted metal that slips to fill it out. In the visualization pool monitoring technique, several aspects should be considered, among them it could be stand out:

Illumination: main responsible for the quality of the input data. The correct illumination is an essential parameter in a computational system vision. In the case of visualization of any welding process, the excessive brightness of the arc voltaic constitutes one of the main problems. One way of reducing that problem is, for instance, to use laser illumination and to capture the image through an optic filter pass-band with center in the laser wavelength [9]. Another way would be to use a filter high-pass band with cutting frequently close to the infrared. The arc brightness has larger intensity close to the ultra-violet range yet the weld pool emits light with frequencies around the infrared [10];

Camera Position in relation to the welding torch: The weld pool shape of the image depends on the camera position and orientation. The ideal position would be visualized from the top, in coaxial orientation to the torch [11]. For this specific orientation, however, it would be necessary to use a special type of welding torch, which would turn the system more complicated and expensive. Since the desirable parameters are the weld pool width, the open root (gap) and the wire distance to the welding joint axis (stand off), the most appropriate position to

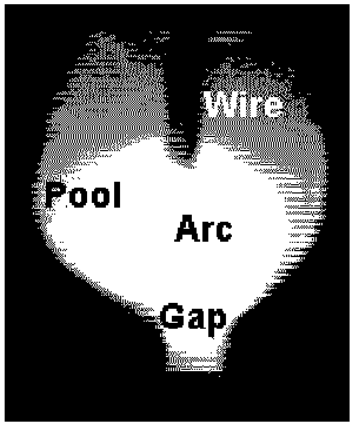

Fig. 1 Frontal image of the weld pool.

achieve that visualization is the front view (figure 2), that allows visualization of gas nozzle, wire, weld pool and joint.

3. Experimental procedure

For the experimental procedure, the following equipments and materials were used:

- Camera CCD Sony XP-999P, with lenses of 50 mm and extension rings (used to increase the focal distance);
- High-pass band optic filter with cutting wavelength close to the infrared;
- Digital frame grabber "Coreco", model "oculos" TCX;
- Inverse power source welding;
- Protection gas (Ar+25%CO2): 12 l/min;
- wire diameter: 0.8 mm;
- Robot ABB IRB2000AW;
- samples in steel plates AISI 1020 with 3,2 mm (1/8") of thickness;

The camera adjustment: shuttering speeds and focal distance of the lens, was carefully studied to reduce the arc reflexes and to obtain an appropriate framing. Figure 2, display the final setup of the several used equipments. The camera holding was projected and specifically fabricated for this work, allowing to change the camera angle in relation to welding torch, as well as to approximate or to move away the camera, allowing better framing and focalization. The welding runs were executed in sequence, varying welding parameters such an as wire feed speed, voltage and distance between the contact tube and the base metal (stand off), in order to changing the weld bead geometry. The objective was to determine the image recognition algorithms performance on extreme cases of very narrow or very wide bead. Other such parameters as welding speed (3,5 mm/s), shielding gas flow (12 l/min), orientation and relative position of camera to the torch, focal distance and the lens shuttering were maintained constant during all the tests.

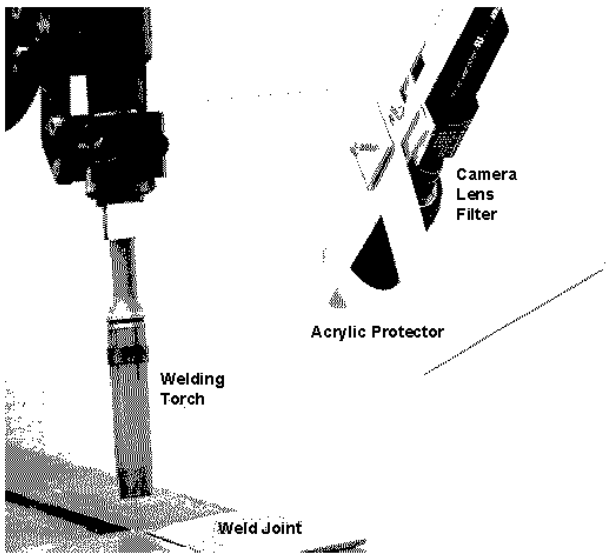

Fig. 2 Final setup of the camera in relation to the welding torch.

Some welds were made bead on plate with the intention of adjusting the camera and the lens for the levels of brightness founded. Others were welding in grove square butt joint, with gap varying from zero to twice the wire diameter, with the objective of determining the detection limits of the weld joint existence coming from the image.

Table 1 Voltage, Wire feed speed and Stand off. Output: weld bead width.

Run	Voltage (Volts)	Wire feed speed (mm/s)	Stand-Off (mm)	Weld bead width (mm)	Gap (mm)
I	18	5	13	2	Bead on plate
II	16	4	13	-	Bead on plate
III	18	5	13	2.5	Bead on plate
IV	19	6	13	3	Bead on plate
V	21	7	13	5	Bead on plate
VI	23	8	13	6	Bead on plate
VII	25	8	13	7	Bead on plate
VIII	27	8	13	6.5	Bead on plate
IX	28	10	13	6	Bead on plate
X	18	5	10	3	1
XI	21	7	10	4	1
XII	23	8	10	5.5	1
XIII	25	8	10	6.5	1
XIV	24.5	10	14	7.6	0.8
XV	24.5	8	14	7.5	0.8
XVI	24.5	8	14	7.4	1.5-0
XVII	24.5	8	14	7.5	1.5-0

The table 1 shows the relationship between the chosen parameters and the weld bead width. During the runs, weld pool images were acquired for developing extraction algorithm of the needed geometric parameters.

4. Developed algorithm

The image processing algorithm consists of two stages: (a) pre-processing and (b) searching algorithm and calculation. The pre-processing algorithm (zoom) is used to select in the image the interest area and its objective is to reduce the pixels amount to be analyzed, decreasing, in this way, the processing time for each frame. The searching algorithm and calculation objective to determine geometric parameters of the pool (maximum width) and gap (width and alignment with the wire).

4.1 Pre-processing - Zoom

In that stage, a zoom is carry out in the interest area inside of the image. The relative position between the camera and the torch is maintained constant, therefore, the zoom is only calculated for the first acquired frame. Those calculations in the image are based in the curve shapes in directions X and Y, as defined in [12 and 13]. It should be observed that, the direction X corresponds to the image lines where the pixels are counting from the left and the direction Y corresponds to the columns in the image, where the pixels are counting from the top.

In the figure 3, it can be observed the profile for one acquired frame. The curves present maximum points, which can be interpreted as corresponding to the area of larger luminous intensity that happens in the electrical arc. Starting from the maximum point of each curve, the coordinates are located in both directions, where the intensity is reduced to a constant minimum value. Those coordinates define the processing window limits. The zoom reduces significantly the amount of bits to be treated by the searching algorithm, reducing the processing time.

4.2 Searching and Calculation

The patterns to search in the image are shown in the figure 4, in that can easily identify the maximum pool width, the gap and the alignment between the wire axis and the joint axis(centralization). However, depending on the moment where the metal transfer cycle is acquired by the digital grabber, it can have variation in the luminous intensity distribution in several areas of interest. That stop the use of threshold technique for weld pool geometry detection [14]. As the illumination is irregular inside of the image (the area of the wire is darker, the pool, brighter and the joint, an area of medium bright), several threshold values for each frame are necessary and vary from frame to frame. Analyzing the Y curve shape and its first and second derivates, it is possible to iden-

tify the Y coordinates of interest image components: the wire, the pool and the weld joint. It should be observed, however, that the profile Y shown in the figure 5 corresponds to the profile Y shown in the figure 3 after applied low-pass band filter, which had for objective to reduce the intrinsic noise to the image capture.

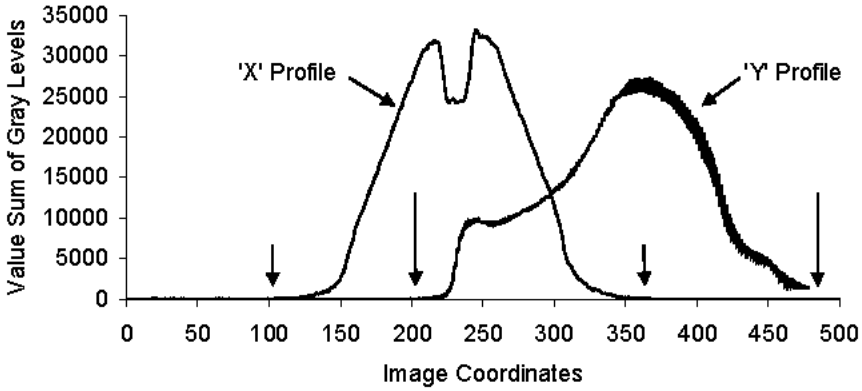

Fig. 3 Profile X and Y of the complete Image, with points indication where the image is cut.

Fig. 4 Image with the measures to be calculated: Weld Pool width, Centralization and Gap width.

Observing the filtered curve (figure 5), it can be noticed that, a concavity change in the position Y corresponding to an image line in that it can be assured the existence of the wire shadow. To detect that concavity change, it is enough to determine the point where the profile second derivate changes of signal. The curve pick of the Y profile (figure 5) indicates the position where the pool has it largest width. The coordinate Y from which the joint becomes visible in the image, it can be obtained by observing the concavity change after the coordinate Y correspond to the pool. Once the lines of the wire, pool and gap are located in the image, the curve distribution analysis of gray levels can be carry on in each of those lines and determine the needed elements X coordinates.

In the identified line for the wire, the figure 6 display the variation of the gray levels with the X coordinate. Observing the curve format, it can be easily placed the wire and establish its width, which is calculated with base in the concavity changes of the curve among the picks, marked with the legends "starting point" and "final point" of the wire. The figure 7, display the gray levels variation in the line corresponding to the maximum pool width in the image. The curve concavity change in its beginning and end permit to identify the beginning and the end of the pool, marked with the legends "starting point" and "final point" of the weld pool.

The figure 8 display the line gray levels variation corresponding to the weld joint in the image. The curve presents a maximum range in that the intensity is approximately constant. The center of this region indicates the joint location and its extension reveal the root opening (gap). This information is obtained by identifying in the curve the concavity change points.

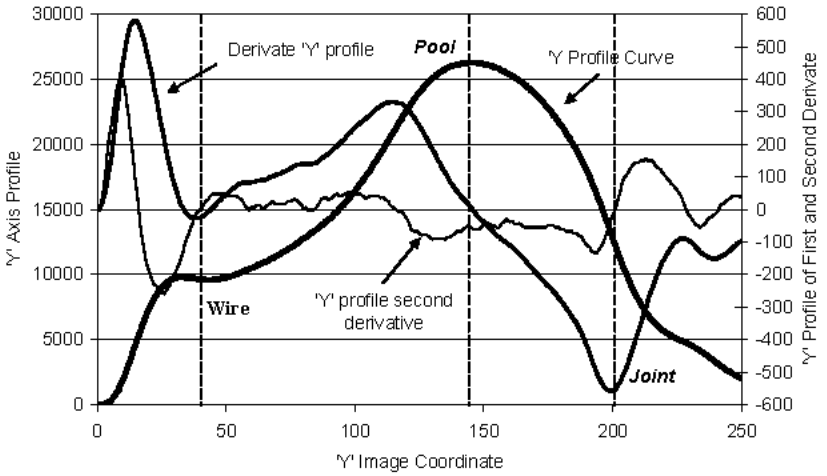

Fig. 5 'Y' Profile of the Reduced Image with Wire Location Indication.

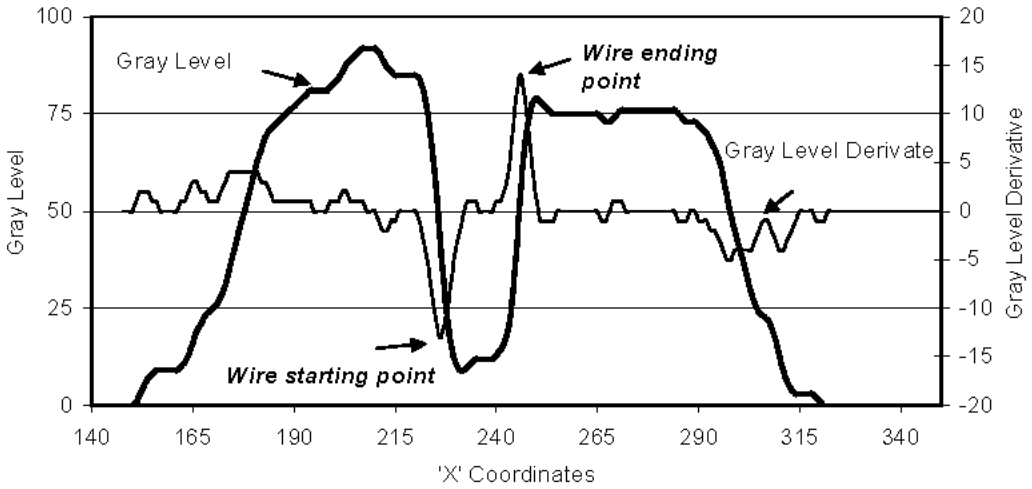

Fig. 6 Gray Level where the wire presence was detected, with indication of initial and final 'X' coordinates positions of the wire.

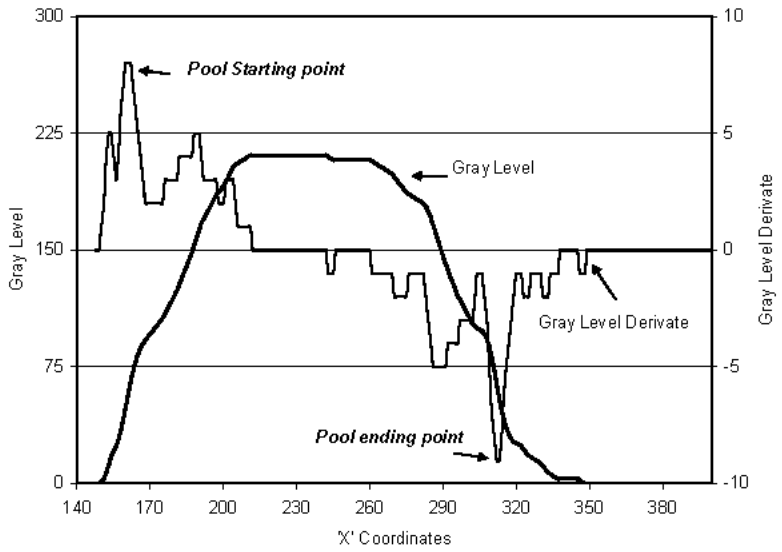

Fig. 7 Gray Level where the pool presence was detected, with indication of initial and final 'X' coordinates of the pool positions.

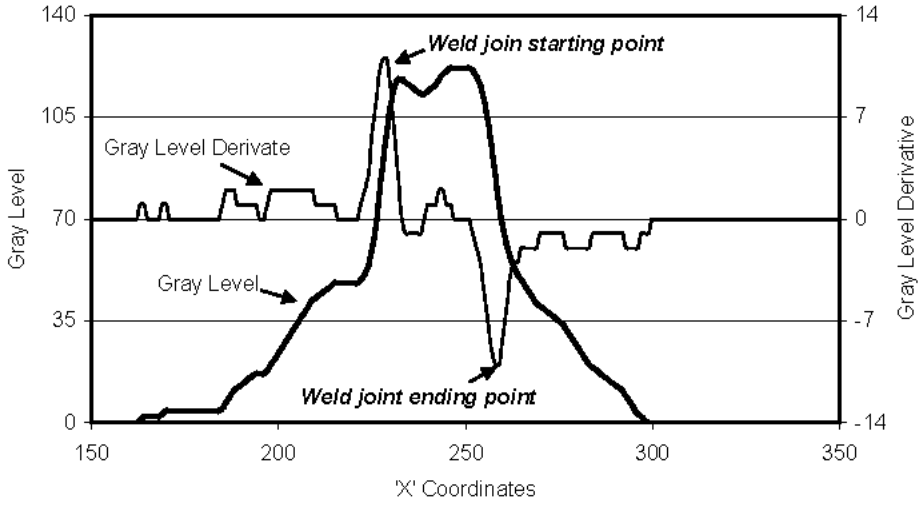

Fig. 8 Gray level in the line where the welding joint presence was detected, with indication of the 'X' coordinate.

5. Results

The developed algorithm was applied to identify the significant parameters (pool width, gap and centralization) from the images collected in the experimental runs. Furthermore, it was measured also the wire diameter and the processing time for each frame. The following results show the 47 acquired frames during the run XI (the table 1). The frames were acquired in sequence with variable period of sampling.

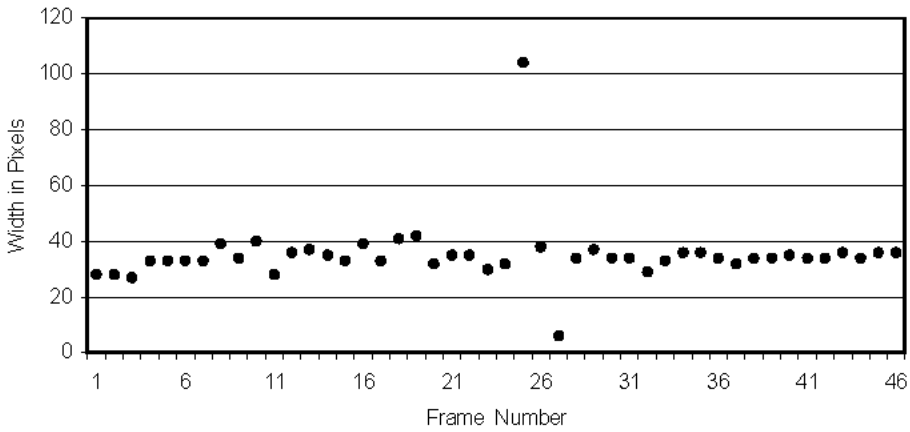

Fig. 9 Wire diameter calculated for the run XI.

As the wire diameter is fixed in all tests (0,8 mm), it can be evaluated its performance by measuring those parameter through the developed algorithm,. The figure 9, display the results of those measurements. The statistical analysis of the frequencies distribution of wire diameter readings shows an index of 47% inside the pixels interval from 33 to 35, that it is the error defined interval for 3,7% in relation to the arithmetic mean of the wire diameter reading values (34 pixels). This average represents the reading expected value for 0,8 mm (for the used focal distance). For larger dimensions than the wire diameter (ex. pool width) it is expected to reach an index of larger success than 47%.

In the same way as above, calculated values curves for the centralization of the wire in relation to the welding joint, gap width ands weld pool width were obtained

The searching algorithm execution time is directly proportional to the image size being processed: as larger the image, more time is necessary for calculate the profile in both axes and to identify the desired parameters. For the 17 run test, the smallest execution time was 50 milliseconds, and the largest 220 milliseconds, with accuracy of 10 milliseconds. As the final objective of the algorithm is the monitoring the welding pool for control ends, it is necessary to assure that the algorithm execution time be the possible smallest. Nevertheless, the algorithm execution time seems reasonable for use in welding bead quality control, if compared to the time constant of the weld pool [15].

6. Conclusions

The developed algorithm presents good results, perceptible when a constant parameter is measured during whole test: the wire diameter. However, that algorithm still shows very sensitive to the adjustments of the camera parameters necessary to reduce the arc reflexes. Considering great variation observed in the times of image processing, it is verified that a commitment exists between the precision that can be gotten with a bigger image and the necessary time to process it.

Acknowledgements

This work was supported by CNPq/RHAE and Finatec.

References

[1] Norrish, J., 1992, Advanced Welding Processes, Institute of Physics, Bristol.

[2] Parmar, R.S., 1995, Welding Processes and Technology, Khana Publishers, Delhi.

[3] Nissley, L., 1983, Understanding positioning errors in robotic arc welding system, Welding Journal, 62(11), pp.30-37.

[4] Kuk, K.A., 1985, Determining acceptable joint mislocation in systems without adaptive control. Welding Journal, 64(11), pp.65-66.

[5] Kurkin, N.S. and Drikker, V.E., 1990, Evaluation of limiting deviations during robotised arc welding T joints. Welding International, 4(7), pp.553-555.

[6] Wadsworth, P., 1987, Assessment of Weld Wire-to-joint Positional Tolerances for Robotic Arc Welding. Edison Welding Institute, Abstract of Report MR8703 (http://www.ewi.org:2001/cgi-bin/cgicookie?dq3re.0.5jn0v9.0.1).

[7] AMERICAN WELDING SOCIETY - SOCIETY OF AUTOMOTIVE ENGINEERS STANDARD: Specification for automotive frame weld quality - arc welding. AWS D8.8-79, SAE HS JII96.

[8] Adolfsson, S. et al., 1999, On line quality monitoring in short-circuit gas metal arc welding, Welding Journal, 78(2), pp. 59s-73s.

[9] Johnson, J. A., Carlson, N.M., Smartt, H.B., Clark, D.E., 1991, Process Control of GMAW: Sensing of Metal Transfer Mode, Welding Journal, April, pp. 91-s – 99-s.

[10] Chen, W., Chin, B.A., 1990, Monitoring Joint penetration Using Infrared Sensing Techniques, Welding Journal, vol. 69(4), pp. 181s-185s.

[11] Richardson, R.W. et al., 1984, Coaxial arc weld pool viewing for process monitoring and control. Welding Journal, 63(3), 43-50.

[12] Galbiati Jr., Louis J., 1990, Machine Vision and Digital Image Processing Fundamentals, Prentice-Hall, New Jersey.

[13] Hall, E. L., 1979, Computer Image Processing and Recognition, Academic Press INC., New York.

[14] Ekstrom, M., 1984, Digital Image Processing and Recognition, Academic Press Inc., Orland.

[15] Carvalho, G.C., 1997, An adaptive Control System for Off-line Programming in Robotic gas metal arc Welding, PhD Thesis, Cranfield University.